PERFORMANCE CHARACTERIZATION, SENSITIVITY AND COMPARISON OF A DUAL LAYER THERMAL PROTECTION SYSTEM

Cole D. Kazemba[(1)]**, Mary Kathleen McGuire**[(2)]**, Austin Howard**[(3)]**, Ian G. Clark**[(4)]**, Robert D. Braun**[(5)]

[(1)] *Daniel Guggenheim School of Aerospace Engineering, Georgia Institute of Technology,*
270 Ferst Drive NW, Atlanta, GA 30332, USA, Email: ckazemba3@gatech.edu

[(2)] *Systems Analysis Branch, NASA Ames Research Center, Moffett Field, CA 94035-0001*

[(3)] *Neerim Corporation, 2551 Casey Ave. Ste. B, Mountain View, CA 94086*

[(4)] *Daniel Guggenheim School of Aerospace Engineering, Georgia Institute of Technology,*
270 Ferst Drive NW, Atlanta, GA 30332, USA, Email: ian.clark@gatech.edu

[(5)] *Daniel Guggenheim School of Aerospace Engineering, Georgia Institute of Technology,*
270 Ferst Drive NW, Atlanta, GA 30332, USA, Email: robert.braun@ae.gatech.edu

ABSTRACT

With the goal of landing high-mass cargo or crewed missions on Mars, NASA has been developing new thermal protection technologies with enhanced capability and reduced mass compared to traditional approaches. Two examples of new thermal protection system (TPS) concepts are dual layer and flexible TPS. Each of these systems introduces unique challenges along with potential performance enhancements. Traditional monolithic ablative TPS, which have been flown on every Mars robotic mission to date, use a single layer of ablative material. The new dual layer TPS concepts utilize an insulating layer of material beneath an ablative layer to increase efficiency and save mass. A study was conducted on the dual layer system to identify sensitivities in performance to uncertainties in material properties and aerothermal environments. A performance metric which is independent of the system construction was developed in order to directly compare the abilities and benefits between the traditional, dual layer and eventually, flexible systems. Using a custom MATLAB code enveloping the Fully Implicit Ablation and Thermal Response Program (FIAT), the required TPS areal mass was calculated for several different parametric scenarios. Overall TPS areal mass was found to be most sensitive to the constraining allowable temperature in each system and aerothermal heat transfer augmentation (attributed here to material surface roughness). From these preliminary results it was found that the nominal dual layer TPS construction investigated could produce improvements over a traditional TPS in the specified performance metric between 14-36%, depending on the flight environments and total integrated heat load expected.

NOMENCLATURE

A&E /A+E – Aerocapture Plus Entry Trajectory
AVCOAT – Ablative Material by Avco for Orion Capsule
CEV – Crew Exploration Vehicle (Orion)
C_P – Specific Heat
FIAT – Fully Implicit Ablation and Thermal
        Response Program
H_{FACT} – Heat Transfer Coefficient
k – Material Conductivity
LI-900 – Silica based insulating material used on Shuttle
MSL – Mars Science Laboratory
ρ – Material Density
PICA – Phenolic Impregnated Carbon Ablator
Q_{SP} – Specific Heat Load
R_C – Contact Resistance
RTV – Room Temperature Vulcanized Adhesive
SIP – Strain Isolation Pad
$T_{Allowable}$ – Allowable Temperature
TPS – Thermal Protection System

1. INTRODUCTION

As the need for landed mass increases from a payload mass of ~1 metric ton (for robotic missions such as Mars Science Laboratory) to 40 metric tons or more (for human exploration class missions), there is an incentive to reduce the mass of the Thermal Protection subsystem (TPS), which traditionally represents a significant fraction of the total system mass. Because heat load scales with entry mass and TPS mass fraction scales with heat load, the incentive is further amplified as the entry mass of the vehicle increases. To date, all Mars entry vehicle designs have used a monolithic ablative TPS for all phases of the trajectory. However, during the low heat flux portions of an entry trajectory, insulating materials are much better suited to protect the vehicle.

One recently developed concept, dual layer TPS, is designed to reduce the mass fraction of the TPS system by tailoring different material layers in the TPS stack to specific portions of trajectory. The dual layer system configuration utilizes an insulating layer (such as Space Shuttle tiles) beneath an ablative layer. This architecture allows the ablative outer surface to be used for the high heat flux portions of a trajectory, for example those that would be seen during an aerocapture maneuver and the first part of an entry phase. Then, after the first layer has fully ablated away the insulative tile beneath acts as the primary defense for the structure during the rest of the entry phase. Thus, ablative material which was previously dispersing energy inefficiently during the low heat flux portion of the trajectory is replaced with a less dense and more efficient insulating tile.

2. QUANTIFYING PERFORMANCE

One of the primary goals of this study was to develop a metric to quantify and compare the performance of not just a dual layer or traditional monolithic TPS, but any thermal protection system. The purpose of developing such a performance metric is to assess TPS design efficiency while including characteristics of the trajectory rather than purely using the masses of the systems. If one were to compare simply the masses of, for example, a monolithic ablative system and a flexible system, no insight would be gained about the trajectory capabilities (or limits) of these systems. In order to capture the ability of a thermal protection system (within a bounded entry class) in regard to both the trajectories it can fly and the TPS mass required to do so, a new TPS performance metric was established. This metric, Specific Heat Load (Q_{SP}), is a ratio of the total integrated heat load seen by the TPS to the required TPS areal mass required to successfully fly a given trajectory while thermally protecting the vehicle.

$$Q_{SP} = \frac{Total\ Integrated\ Heat\ Load}{Total\ TPS\ Areal\ Mass} \qquad (1)$$

It is useful to think of this new performance parameter as analogous to specific impulse used in propulsion. Specific impulse is a ratio of the total change in momentum achieved per unit weight of propellant. Similarly, the units of Q_{SP} (kJ/kg) reveal that it is a ratio of the amount of energy which can be sustained at a given location on the vehicle per unit mass of the TPS. This parameter allows greater versatility in comparison of different thermal protection systems because it combines the 'performance' of the TPS (heat load) with its mass. It is this performance metric which was used for comparison of the traditional and dual layer systems in this study.

3. STRATEGIC APPROACH

3.1 Test Case

The test case used for this study came from NASA's 2009 Mars Entry, Descent and Landing Systems Analysis Study [4], [5] and consisted of a mid L/D, rigid aeroshell vehicle on a dual heat pulse trajectory. The first pulse is designed to slow the vehicle from its hyperbolic approach trajectory to a parking orbit via aerocapture within Mars' atmosphere. Following a long on-orbit cool off period, the vehicle would then perform an entry maneuver through the atmosphere and descend down to the Martian surface. Fig. 1 shows the vehicle geometry with contours indicating the total integrated heat load for the aerocapture plus entry mission. This study focused on locations with five different integrated heat load values which are highlighted in the legend. Fig. 2 shows the heat flux seen by the vehicle for each of the two pulses through the atmosphere and Fig. 3 presents a schematic showing the key events of the reference trajectory.
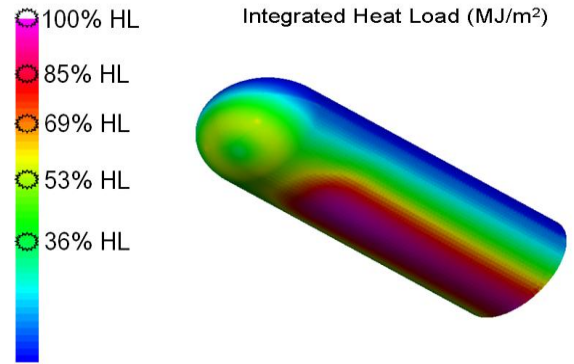

Fig. 1. The mid L/D, rigid aeroshell vehicle with contours of total integrated heat load shown. The five different colored contours represent the heat load environments investigated in this study.
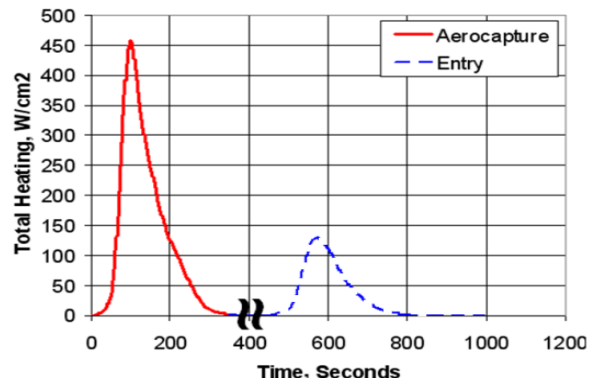

Fig. 2. The associated, fully margined, heating as a function of time for the two pulses through the atmosphere.
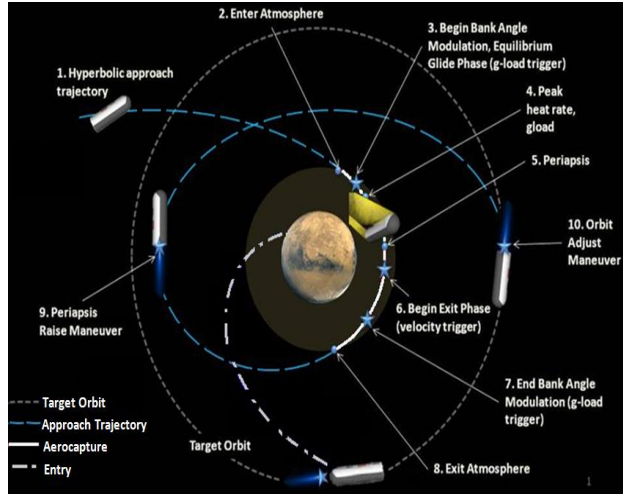
Fig. 3. A schematic of the events leading from the hyperbolic approach trajectory to landing on the Martian surface [4].

3.2 Sizing Approach

To determine the required thickness of each layer for a given node on the vehicle, a three step sizing optimization process was used for the dual layer system [5]. The stack of materials modeled consisted of an ablator (either PICA or Avcoat) on top of LI-900 Shuttle insulative tile, followed by a mutli-layer substructure with a Strain Isolation Pad (SIP) in between two Room Temperature Vulcanized (RTV) adhesive layers and a Titanium carrier structure. For the first step, only the entry portion of the trajectory was run with the insulator as the only protecting material on top of the RTV-SIP-RTV-Titanium substructure of the vehicle. In this step, the insulator was sized in order to maintain the maximum temperature of the adhesive (RTV) to its nominal allowable threshold value of 560 K. Next, keeping this thickness of the insulating layer, the entire aerocapture and entry trajectory was simulated with an ablator on top of the insulator. In this case, the ablator was sized such that the maximum temperature of the insulator surface was equal to its maximum nominal allowable temperature (1700 K for LI-900). The constraining material temperature limit for an iteration of the optimization process is referred to as the "maximum backwall temperature". Finally, the whole trajectory was simulated again with the optimized thickness of the ablator now remaining constant while the insulator thickness was re-optimized to keep the RTV maximum temperature at its 560 K threshold. This final step trimmed some of the allocated insulator from the initial entry-only calculation and resulted in an optimized TPS stack for the given constraints. Fig. 4 depicts this sizing process.
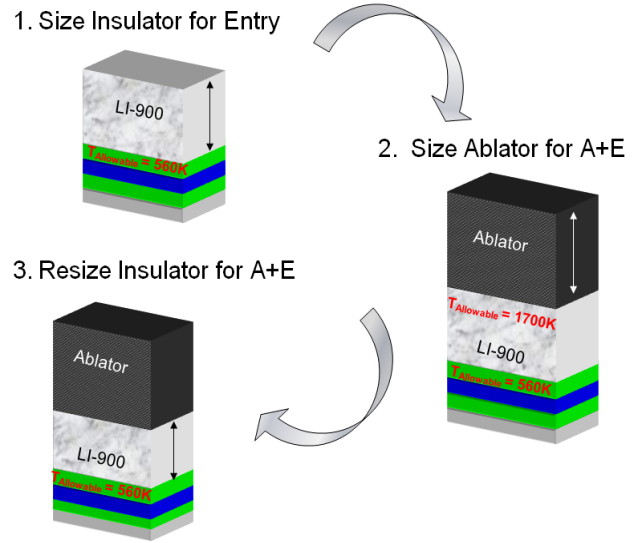

Fig 4. A schematic of the dual layer sizing process. The first step sizes the insulator (LI-900) to protect the RTV for entry. Next, using the resulting LI-900 thickness, the ablator is sized to protect the LI-900 surface throughout both aerocapture and entry. Finally the LI-900 is resized to protect the RTV for the whole trajectory with the optimized ablator thickness on top

The sizing process described in Fig. 4. is applied with the nominal values to establish a baseline. Then, the sensitivities to the aerothermal environment and various material properties of the ablative and insulating materials were determined by varying the properties within their 3 sigma uncertainty bounds and observing the impact on the final areal mass of the system. Table 1 summarizes all of the variables and sizing scenarios examined in this study.

Table 1. A summary of the sizing scenarios investigated. Note: the virgin and char properties of the ablators were varied in unison

Dual Layer TPS Sizing Scenarios			
Material sized	Material Varied	Properties Varied	Trajectory
LI-900	LI-900	C_P, k, ρ, H_{FACT}	Entry
PICA	PICA	$C_P, k, \rho, H_{FACT}, R_C$	Aerocapture
PICA	PICA	C_P, k, ρ	Aerocapture and Entry
PICA	LI-900	$C_P, k, \rho, T_{Allowable}$	Aerocapture and Entry
LI-900	LI-900	C_P, k, ρ	Aerocapture and Entry
LI-900	PICA	C_P, k, ρ, H_{FACT}	Aerocapture and Entry
AVCOAT	AVCOAT	$T_{Allowable}, k, \rho, H_{FACT}$	Aerocapture and Entry
LI-900	AVCOAT	k, ρ, H_{FACT}	Aerocapture and Entry

Traditional Monolithic TPS Sizing Scenarios			
Material sized	Material Varied	Properties Varied	Trajectory
PICA	PICA	$T_{Allowable} \rho, k, H_{FACT}, R_C$	Aerocapture and Entry
AVCOAT	AVCOAT	$T_{Allowable} \rho, k, H_{FACT}, R_C$	Aerocapture and Entry

3

The insulator used throughout the entire study was the LI-900 shuttle tile. The primary ablator used was Phenolic Impregnated Carbon Ablator (PICA) which has flight heritage on the Stardust sample return mission and will be used for the heat shield of the Mars Science Laboratory (MSL) mission scheduled to launch in 2011. A second ablator, Avcoat, was investigated in a more limited sense for comparison. Avcoat is the baseline ablative TPS for the Orion CEV heat shield.

3.3 Computational Approach

The ablation and thermal analysis tool used to perform the extensive calculations needed to capture the complex physics involved during atmospheric entry was the Fully Implicit Ablation and Thermal Response Program (FIAT) [3]. In order to carry out the high volume of input file modifications, FIAT simulations, data organization, and post processing, a custom MATLAB™ architecture was constructed around FIAT. The program takes inputs from the user such as the desired trajectory and an initial thickness guess, as well as the material or environmental parameter of interest and the uncertainties associated with that variable. These inputs are then used to reconstruct the FIAT main, environment and material database input files. Next the MATLAB program launches FIAT which executes the transient thermal ablative analysis and returns the resulting temperature and heat flux profiles seen through the depth of the material stack.

In addition to streamlining the sizing process steps, the MATLAB program was also used to implement a convergence criteria which varied slightly from the one built into FIAT for the dual layer cases. This was required for the ablator sizing portion of the process because FIAT was not designed to optimize an ablator thickness for a system in which the ablator is completely ablated away before the end of the transient analysis (i.e. the ablative material reaches zero thickness). When the ablator is completely ablated away, a spike in the insulator surface temperature is observed. This spike can be attributed primarily to two factors: the decrease in emissivity when the exposed surface changes from ablator (virgin or charred) to LI-900 and a thinning of the boundary layer due to the lack of blowing effects which are induced by the ablation products. Fig. 5 shows the LI-900 surface temperature at various PICA densities for the entry portion of a full trajectory with a dual layer system. The max temperature (occurring at the peak of the spike following full ablation) is constrained to the material limit of LI-900 (1700 K).

As shown in Fig. 5, the insulator surface temperature spike following ablation may exceed the peak temperature that the insulator experienced prior to full ablation. The current version of FIAT will optimize the ablator to maintain the insulator temperature for the first peak, but not the second. In order to ensure that the ablator is optimized to maintain the tile surface allowable temperature throughout both the pre-ablation maximum and the post-ablation spike, a custom optimization process was implemented via MATLAB and used instead of FIAT's built in optimizer for sizing the ablator.
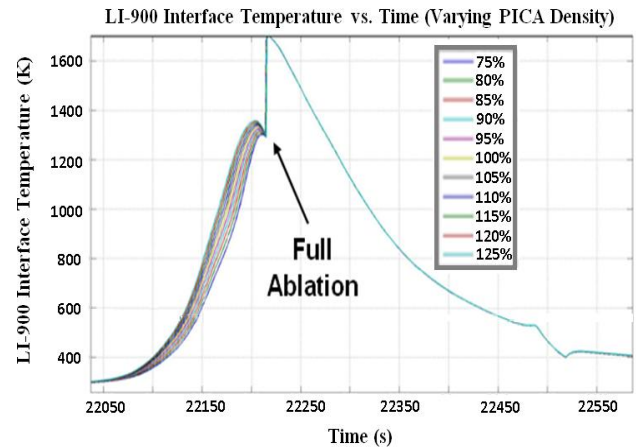

Fig. 5. LI-900 Surface Temperature vs. Time for the entry portion of a full trajectory with varying PICA density.

The process is as follows. If the maximum temperature experienced beneath the material being sized is greater or less than its nominal allowable temperature, the MATLAB script varies the thickness appropriately and relaunches FIAT. This is repeated until the maximum backwall temperature equals the specified value. A schematic of this process is shown below in Fig. 6.
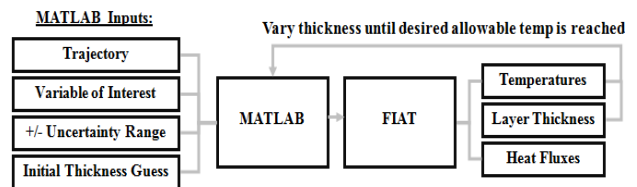

Fig. 6. A schematic of the computing approach used to obtain the results of the study.

4. RESULTS

Each of the scenarios presented in Table 1 were analyzed with the previously described approach for a node on the vehicle which experiences 85% of the total integrated heat load. Then, areal mass sensitivities for each variable were obtained for both the traditional and dual layer

systems. From this information, the variables to which the systems were most sensitive were identified. Next, the remaining four nodes were subject to the performance characterization process in order to see how their areal masses depended on changes in the key variables identified. Finally, with tabulated ranges of areal mass at each of the five heating conditions considered for each variable, variance in the performance metric could be calculated. Table 2 lists the uncertainty values used in the study. The performance as a function of independent changes in the key parameters was then compared and conclusions about performance and sensitivity in the two systems were drawn.

Table 2. Uncertainty values used in this study.
[1], [2], [6]

Property	2σ Unc.	3σ Unc.
PICA		
Density (kg/m^3)	7.50%	11.25%
Specific Heat (J/kg-K)	5.00%	7.50%
Conductivity (W/m-K)	15.00%	22.50%
Surface Roughness	15.00%	22.50%
RTV Allowable Temp. (K)	10.00%	15.00%
LI-900		
Density (kg/m^3)	7.50%	11.25%
Specific Heat (J/kg-K)	7.50%	11.25%
Conductivity (W/m-K)	1.50%	2.25%
Allowable Temp. (K)	10.00%	15.00%

4.1 Areal Mass Sensitivities

Before the performance metric could be applied to the systems, areal mass variations due to perturbations in the environmental and material properties needed to be calculated. First, the nominal values were calculated for the dual layer and monolithic systems. Then, varying one parameter at a time within the expected 3 sigma range of values, areal mass variations were found. The results of this process are summarized using plots of the required areal mass for the layer being sized versus variations in the parameter from its nominal value.

4.1.1 Dual Layer Results

Figs. 7-9 summarize the results from the three variables which had the greatest impact on areal mass for the dual layer system. These results were combined with any associated system mass changes due to coupling effects and the substructure mass to obtain the minimum and maximum areal masses of the *total* thermal protection system. Where applicable, the vertical lines plotted depict the ± 2σ and ± 3σ uncertainties in the variable of interest.

From the dual layer results it can be seen in Fig. 7 that the overall range of values for areal mass are most influenced by changes in the heat transfer coefficient due to surface roughness of the PICA. Based on estimates from previous studies with PICA for the Mars Science Laboratory heat shield [1], the 3σ uncertainty was estimated to be 22.5%. Further measurements from arc jet test articles are required to better understand this uncertainty. This relationship appears to very linear with a slight change in slope at 85% of the nominal. The surface roughness parameter also had a significant coupling effect on the required LI-900 thickness beneath the ablator. This coupling was used in calculating the final TPS areal masses and performance metrics.

The second most important variable in terms of areal mass sensitivity was the allowable surface temperature of the LI-900 insulator. This value was scaled by ±15% based on arc jet tests results from a similar insulator (LI-2200) which suggest the material could survive temperatures upwards of 1900 K [2]. Looking at Fig. 8 it can be seen that if a material was used with a lower allowable temperature than LI-900, the required PICA to protect the structure increases, as expected. However, it can be seen that as the allowable temperature of the LI-900 is allowed to increase, there is a sharp decrease in the PICA areal mass required. This is attributed to the fact that at the higher allowable temperatures, the insulator begins to approach a point where it no longer needs the ablator to protect it during the second (entry) heat pulse. With just a 15% increase in allowable temperature of the LI-900, the required areal mass of PICA is lowered by 50%.
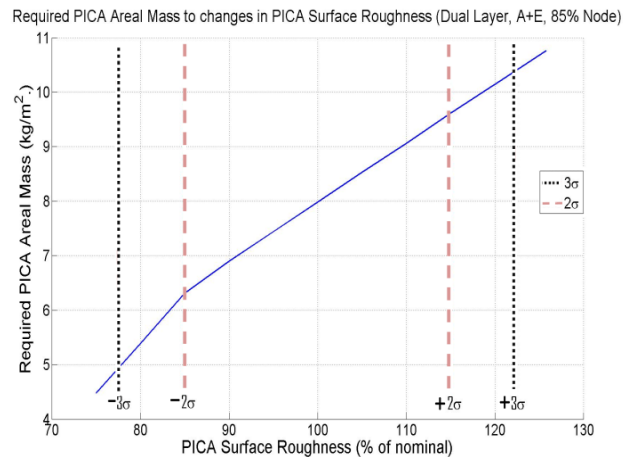

Fig. 7. Required areal mass of PICA with variations in the PICA surface roughness for a dual layer system. The vertical dashed lines represent the ± 2σ and ± 3σ uncertainties in the surface roughness heating augmentation.
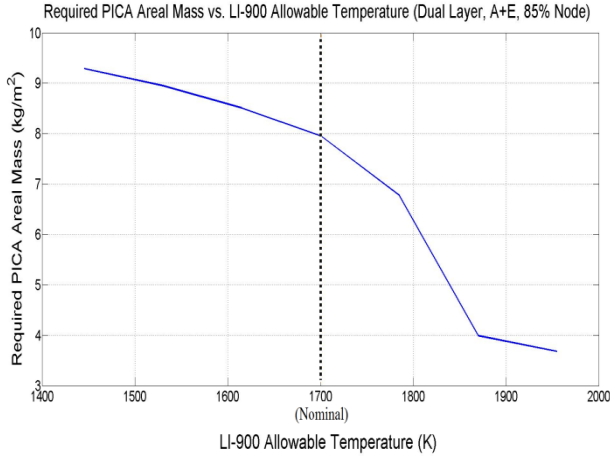
Fig. 8. Required areal mass of PICA with variations in the LI-900 allowable surface temperature.

Fig. 9 highlights the dependence of required LI-900 aeral mass to changes in LI-900 density from its nominal value. It can be seen that there is a positive linear correlation between the density and the required areal mass (i.e. with increasing density of the material, the required areal mass increases). This dependence is opposite to the more intuitive negative correlation between the density and the required *thickness* (i.e. with increasing density of the material, the required thickness decreases). The reason for the trend reversal is that areal mass is a function of thickness *and* density. Thus, a change in required thickness and the accompanying change in material density must both factored into the required areal mass. Therefore, as the LI-900 density increases, the required areal mass also increases, even though the required thickness decreases. In the case of LI-900 there is not a large change in required thickness as its density changes, but since its density is changing by a significant amount ($\pm$ 3σ), the resulting required areal mass has a relatively strong dependence on LI-900 density.
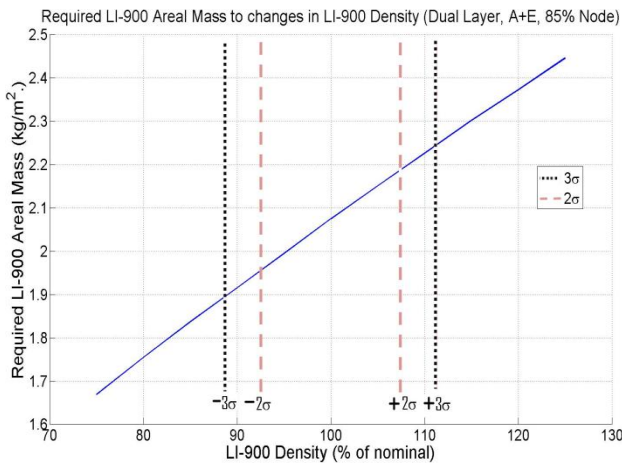

Fig. 9. Required areal mass of LI-900 with variations in LI-900 density.

4.1.2 Single Layer Results

Figs. 10-13 present the areal mass sensitivities for the monolithic PICA TPS. The first thing to note is the significant increase in the nominal value for required PICA areal mass compared to the dual layer system ($\approx$12.8 kg/m^2 for the single layer system and $\approx$8 kg/m^2 for the dual layer). Although there is an offset in the nominal values, the areal mass of the traditional system was also most sensitive to changes in the surface heat transfer coefficient (referred to as surface roughness) and the allowable temperature of the layer beneath the PICA (Figs. 10 and 11, respectively). The nominal allowable temperature constraint here is the 560 K specified limit for RTV.

Unlike the dual layer system where the relationship between the allowable backwall temperature (the 1700 K limit for LI-900) and required areal mass was quite non-linear, in this construction the required ablator varies smoothly with changes in the RTV allowable temperature.
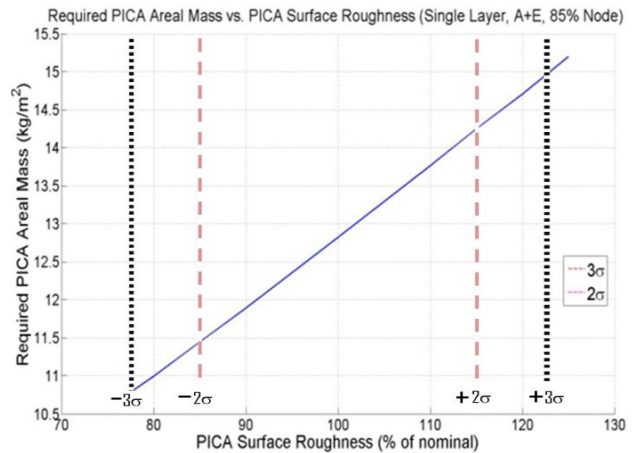

Fig. 10. Required areal mass of PICA with variations in the PICA surface roughness for a monolithic system

The other two variables which had a significant impact on the required PICA in the monolithic construction were the conductivity and density of the PICA (Figs. 12 and 13, respectively). Both of these variables had a much greater impact in the single layer case than the dual layer. As with the density of the insulator in the dual layer case, the required *thickness* of PICA due to changes in its density varies opposite to the required areal mass. However, as opposed to the LI-900 behavior, the required thickness varies greatly with changing density (almost a 50% change in the plotted range of $\pm$25% of the nominal density). However, when combining this change in thickness with the associated density, the percent variance in areal mass is significantly less sensitive to the ablator density than it was the LI-900 density, although still appreciable.
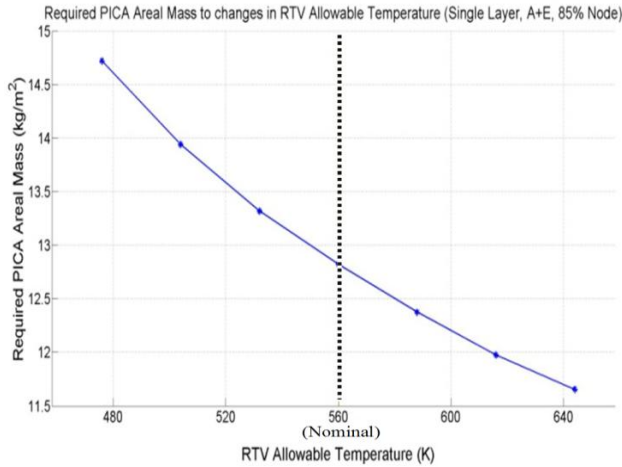
6

Fig. 11. Required areal mass of PICA with variations in the RTV allowable temperature.
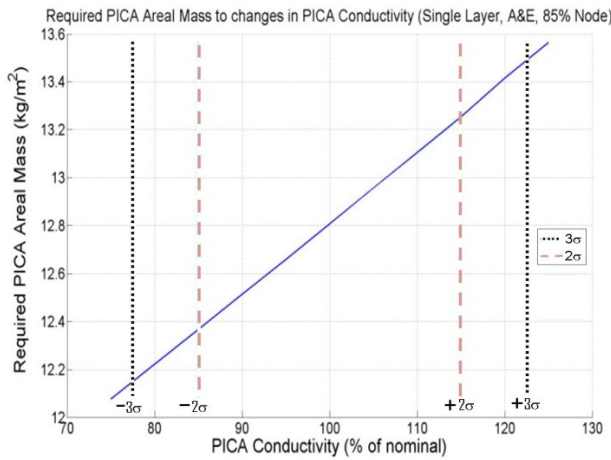

Fig. 12. Required areal mass of PICA with variations in the PICA conductivity.
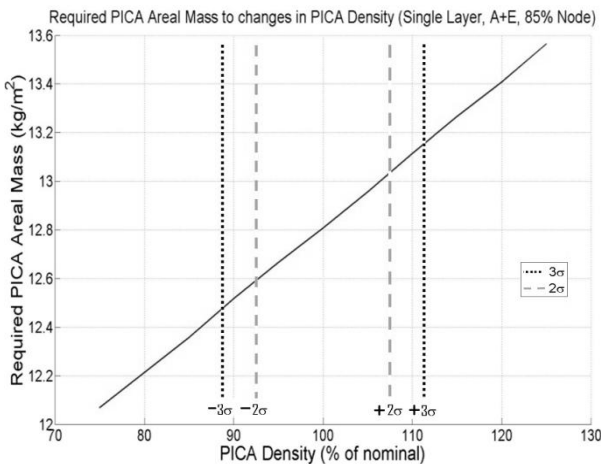

Fig. 13. Required areal mass of PICA with variations in the PICA density.

4.1.3 Summary

Combining the results discussed above with any coupling effects and the substructure construction, the impact of the uncertainties in each variable on the total areal mass of the TPS can be calculated. It is this final areal mass of each complete system which is used in calculating the Specific Heat Load performance metric. Table 3 summarizes the parameters which produced the greatest performance variance for both the dual and single layer systems at the 85% heat load node. In addition to the plotted variables of surface roughness, LI-900 allowable temperature, and LI-900 density, dual layer results for the PICA conductivity and density are also tabulated here for comparison to the single layer system. It can be seen that the uncertainties in the PICA conductivity and density have an order of magnitude greater impact on the single layer system than the dual layer system.

Table 3. A summary of the most significant variables in for the 85% heat load node for both the dual layer and single layer systems.

Dual Layer: Key Areal Mass Sensitivities for 85% Heat Load					
Rank	Layer Sized	Trajectory	Varaible	Min Areal Mass (% of nominal)	Max Areal Mass (% of nominal)
1	PICA	A&E	Surface Roughness	85.70%	114.14%
2	PICA	A&E	LI-900 Allowable Temp	81.90%	103.92%
3	LI-900	A&E	LI-900 Density	99.21%	100.81%
4	PICA	A&E	PICA Conductivity	99.46%	100.38%
5	PICA	A&E	PICA Density	99.68%	100.16%

Single Layer: Key Areal Mass Sensitivities for 85% Heat Load					
Rank	Layer Sized	Trajectory	Varaible	Min Areal Mass (% of nominal)	Max Areal Mass (% of nominal)
1	PICA	A&E	Surface Roughness	89.73%	110.27%
2	PICA	A&E	RTV Allowable Temp	95.48%	104.52%
3	PICA	A&E	PICA Conductivity	96.72%	103.28%
4	PICA	A&E	PICA Density	98.35%	101.65%

4.2 Specific Heat Load Sensitivities

Taking the results summarized in Table 3 and combining them with the total integrated heat load seen at the 85% node, the Specific Heat Load, Q_{SP}, can be calculated. It is this value which is used to compare the two different systems analyzed in this study and would be used in future work to compare other systems, such as flexible TPS.

4.2.1 85% Node Only

Plotted in Fig. 14 is the performance metric for both the dual layer and monolithic systems for the 85% heat load case as a function of ±3σ variance in the previously identified key parameters. The Specific Heat Load is plotted on the y-axis. Increasing values represent improving performance. The vertical bars represent the range in performance values observed when the specified parameter was varied between its ± 3σ values.
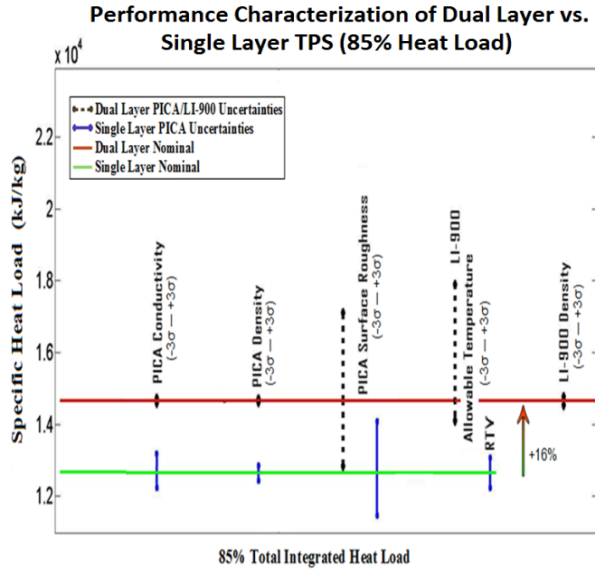
Fig. 14. Variations in Q_{SP} with variations in key parameters from their -3σ to +3σ uncertainty values. The solid horizontal lines represent the nominal performance for the dual layer and single layer systems. Performance variations from the nominal due to parameter uncertainties are shown with the vertical bars.

The same trends discussed in the areal mass sensitivities can be observed in this plot. The dual layer system is less sensitive to material properties than the traditional monolithic system and both systems are most sensitive to the surface roughness heat augmentation and the allowable temperature of the ablator backwall. Note the 16% increase in nominal performance of the dual layer system over the traditional system.

4.2.2 Five Reference Heat Loads

When looking at results from only one reference node, one can see how changes in each variable impact the performance of the TPS at that specified heating condition. In Fig. 15, the performance trends and sensitivities for each of the five heat loads investigated are plotted. The data for 85% heat load shown here is the same as in Fig. 14, however, when this data is shown along with data from other heating conditions, conclusions about the relationship between heat load, performance, and sensitivity can be drawn.

With increasing heat load the absolute performance for each system increases. This is due to the fact that PICA operates more efficiently in a higher heating environment. The changes in absolute performance with varying heat loads presents an opportunity to utilize the specific heat load performance metric for material selection purposes. In a block construction heat shield, each cell on the heat shield could be easily tailored with different materials at different locations depending on the

expected heating environment at the corresponding location on the body [7].

The amount of deviation from the nominal values as a function of heat load provides information about the sensitivity in each environment. In the dual layer system there is consistent increases in sensitivity to surface roughness and LI-900 allowable temperature as the heat load increases from 36% up to 100% of the total. In the single layer case, the variation in expected performance increases with increasing heat load primarily for the surface roughness. Sensitivities to the density and conductivity of both PICA and LI-900 remain fairly constant as heat load changes for both constructions.
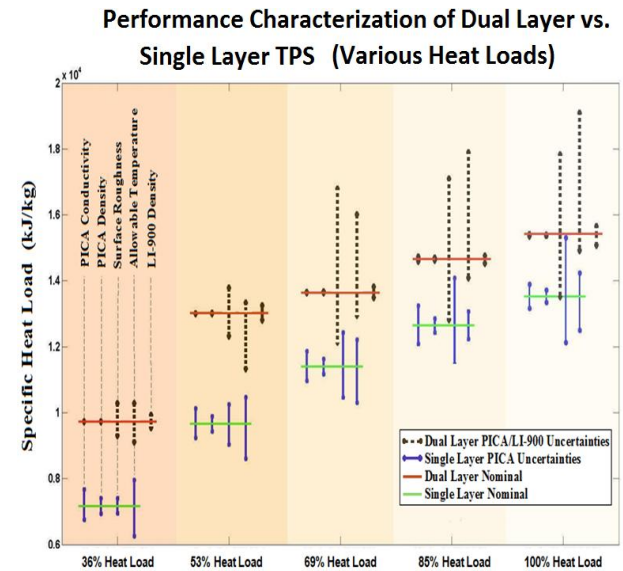

Fig. 15. Variations in Q_{SP} with variations in key parameters from their -3σ to +3σ uncertainty values for all heat loads investigated.

4.2.3 Root Sum Squared Data

If the data for each system at each node is combined by taking the Root Sum Square (RSS) of all of the deviations from the nominal due to each variable, the clusters of vertical bars from Fig. 15 can be collapsed into one. This depiction of the data paints the whole picture about the ranges of performance that can be expected for each scenario. Also, with a more condensed version of the data, it is easier to compare the relative benefit the dual layer system for each heating environment. Fig. 16 shows the RSS uncertainties in performance and the relative increase in nominal performance for the dual layer system for each heat load. As the heat load increases, the relative benefit decreases from 36% in the lowest heating environment to 14% for the maximum integrated heat load. At the same time, the overall variability in the systems increases with increasing heat

load. This implies that the performance of the TPS is significantly more sensitive to environmental and material parameters when it is subject to extreme heating.

Knowledge of the heat load dependence of both the overall performance and its sensitivity to uncertainties provides significant insight for future TPS design. Because the absolute performance of the monolithic and dual layer systems decays at lower heat loads, material selection might be guided so as to optimize the specific heat load at each location of the body. This could be suited towards a heat shield with cellular construction [7] so the optimization could be conducted with high resolution (as opposed to the large TPS segments in the heat shield of MSL, for example). The sensitivity of the performance at each heating condition can be used to find TPS materials with better understood and consistent material properties than some of the ablators used currently. A material which may have a lower nominal absolute performance than other competing possibilities may still result in an overall lighter TPS due to the decrease in required margin.
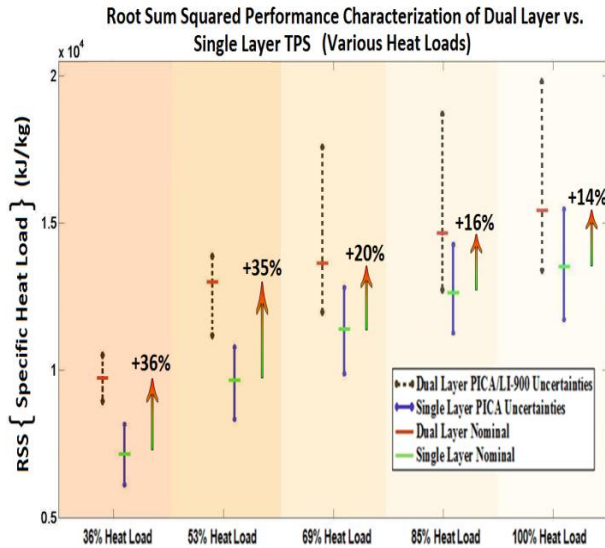

Fig. 16. RSS variations in Q_{SP} for each heat load investigated. With increasing heat load there is decreasing relative benefit of the dual layer system over the single layer and increasing uncertainty.

4.3 Avcoat Comparison

As was briefly mentioned in Section 3, a second ablator was investigated in both a dual layer and single layer configuration for comparison to PICA. This second ablator, Avcoat (the material chosen for the Orion heat shield), was analyzed for the 85% heat load environment. While the sensitivity trends between the two different ablators are relatively similar (with the exception being

increased sensitivities to ablator density and conductivity), what is truly of interest here is the relative performance of the two Avcoat systems to their PICA counterparts. Fig. 17 is a plot of the Specific Heat Load for these four systems at 85% of the total heat load. Comparing the horizontal nominal line of the dual layer Avcoat/LI-900 system to the nominal line representing the dual layer PICA/LI-900, it is clear to see that the TPS performs significantly better with PICA as the ablative material (≈28% increase in performance) rather than Avcoat. Looking at the single layer systems, a similar trend between the single layer Avcoat nominal and the single layer PICA nominal is observed (≈30% increase in performance with PICA versus Avcoat). It is clear that for this trajectory and this heating environment, PICA is the more efficient ablative material.
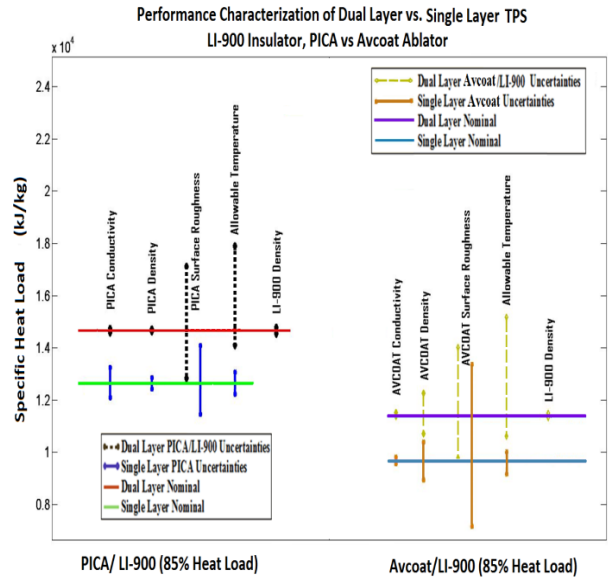

Fig 17. Performance of the dual layer and single layer systems with 85% heat load for two different ablators.

5. CONCLUSIONS

A study was conducted with a new dual layer thermal protection system and a traditional monolithic TPS to correlate sensitivities in performance to uncertainties in material properties and aerothermal environments. A performance metric, Specific Heat Load, was developed in order to directly compare the results of the traditional, dual layer and eventually, flexible systems. This metric takes into account both the heat load seen by TPS and the required areal mass of the system to withstand this heat load. A custom MATLAB code was created around the Fully Implicit Ablation and Thermal Response Program (FIAT) to calculate the required TPS areal mass for several different scenarios. Overall TPS areal mass was found to be most sensitive to the heat transfer augmentation due to surface roughness and the allowable

temperature at the backwall of the ablator. The variations in areal mass for each case were combined with the heat load to get variations in the Specific Heat Load performance metric. Overall sensitivity in performance increased with increasing heat load for both systems. The relative nominal performance benefit of the dual layer system is substantial across the board, but decreases as the heat load increases. At the lowest heat load investigated here, the relative benefit was a 36% improvement in performance and at full heat load the advantage was 14%. Finally, Avcoat was investigated for one heating environment in order to compare its performance to that of PICA in both a dual layer and traditional configuration. In both cases the PICA significantly out-performed the Avcoat for this particular application.

6. FUTURE WORK

There are several future tasks which would provide further insight into the performance potential and sensitivity of various thermal protection systems. The Specific Heat Load metric introduced in this study would allow for easier comparisons of vastly different TPS systems which have the same overall mission. For example, applying the performance analysis laid out in this study to a flexible TPS would allow for the application of the performance metric to show its true value by doing a direct comparison of a rigid TPS to an inflatable decelerator utilizing a flexible TPS and flying a starkly different entry trajectory. In addition to flexible systems, much could be learned from investigating other constructions such as an ablator-ablator dual layer system.

The approach to performance optimization may also benefit from changes. Possibilities range from investigating a wider variety of parameters, varying virgin and char properties of the ablator independently and sizing without allowing full burn-through of the ablator.

Work is currently being done to better quantify the amount of surface roughness which occurs on the materials in question and the associated heating augmentation, which was shown to be the most important variable regarding performance sensitivity.

Finally, with a complete understanding of the performance characteristics of each TPS, development risk and reliability assessments for each system would provide a comprehensive picture for each option. This would allow decisions to be made about which system or systems are best suited towards achieving the ultimate goal of increasing the landed mass capability of future missions.

7. REFERENCES

1. K.T. Edquist, A.A. Dyakonov, M.J. Wright, and C.Y. Tang. "Aerothermodynamic Design of the Mars Science Laboratory Heatshield," AIAA Paper 2009-4075. AIAA Thermophysics Conference, San Antonio, Texas, June 2009.

2. J. Heinemann, H Goldstein. Silica Impregnated Refractory Ceramic Ablator (SIRCA) Arc Jet Test Report," November 2006.

3. Y.K. Chen and F.S. Milos, "Ablation and Thermal Response Program for Spacecraft Heatshield Analysis," *Journal of Spacecraft and Rockets*, Vol. 36, No. 3, 1999, Pp. 475-483.

4. Dwyer-Cianciolo, A. M., et al., "Entry, Descent and Landing Systems Analysis Study: Phase 1 Report", NASA/TM-2010-216720, July 2010.

5. M.K. McGuire, "Dual Heat Pulse, Dual Layer Thermal Protection System Sizing Analysis and Trade Studies for Human Mars Entry Descent and Landing," AIAA-2011-343, 49th AIAA Aerospace Sciences Meeting, Orlando, FL, 4-7 January 2011.

6. Wright M., "CEV Thermal Protection System (TPS) Margin Management Plan," NASA-ARC, C-TPSA-A-DOC-7005, Rev. 2.0, Nov. 12, 2009.

7. Zell, P. T., Venkatapathy E., and Arnold, J. O., "The Block-Ablator in a Honeycomb Heatshield Architecture," 7th International Planetary Probe Workshop, Barcelona, Spain, June 12-18, 2010.